Non-Invasive Load Monitoring of Induction Motor Drives Using Magnetic Flux Sensors

Zheng Liu [1], Guiyun Tian [1], Wenping Cao [2*], Xuewu Dai [3], Brian Shaw [4], Robert Lambert [4]

[1] School of Electrical and Electronic Engineering, Newcastle University, Newcastle upon Tyne, United Kingdom
[2] School of Engineering and Applied Science, Aston University, Birmingham, United Kingdom
[3] Department of Physics and Electrical Engineering, Northumbria University, Newcastle upon Tyne, United Kingdom
[4] Design Unit, Newcastle University, Newcastle upon Tyne, United Kingdom

Abstract: Existing load monitoring methods for induction machines are generally effective, but suffer from sensitivity problems at low speeds and non-linearity problems at high supply frequencies. This paper proposes a new non-invasive load monitoring method based on giant magnetoresistance (GMR) flux sensors to trace stray flux leaking from induction motors. Finite element analysis (FEA) is applied to analyse stray flux features of test machines. Contrary to the conventional methods of measuring stator and/or rotor voltage and current, the proposed method measures the dynamic magnetic field at specific locations and provides time-spectrum features (e.g. spectrograms), response time load and stator/rotor characteristics. Three induction motors with different starting loading profiles are tested at two separate test benches and their results are analysed in the time-frequency domain. Their steady features and dynamic load response time through spectrograms under variable loads are extracted to correlate with load variations based on spectrogram information. In addition, the transient stray flux spectrogram and time information are more effective for load monitoring than steady state information from numerical and experimental studies. The proposed method is proven to be a low-cost and non-invasive method for induction machine load monitoring.

Index Terms – Giant magnetoresistance (GMR), induction motor drives, load monitoring, magnetic flux, measurement, sensors, stray flux.

Corresponding Author:

Prof. Wenping Cao

School of Engineering and Applied Science, Aston University

Birmingham, United Kingdom

Tel: +44 (0)121 2044264

Email: w.p.cao@aston.ac.uk

1. Introduction

Induction motor drives play an important role in many industrial applications from a few watts to several megawatts, and they consume the majority of electricity used by industry [1, 2]. During their service life, the operational costs can easily be in excess of their capital costs. In order to increase their reliability and energy efficiency, monitoring their operational conditions is of critical importance. In particular, load anomalies have an impact on machine operation and power quality. Additionally, variable loads can cause ambiguity or misinformation in a machine condition monitoring system [3]. For load monitoring, a non-invasive method without any torque sensors is attractive especially in harsh environments [4]. Hence, this work develops a state-of-the-art condition monitoring technique based on magnetic flux sensors.

In general, the torque monitoring procedure is based on simplified induction machine models for steady-state and quasi-steady-state analysis. Simulation studies use dynamic models of induction machines followed by experimental measurements [5]. Torque transducers for non-invasive measurements with multiple functions are still a challenge for researchers [5]. Some electrical methods are based on the measurements of electrical terminal quantities such as voltage and current. Motor current signature analysis (MCSA) is popular which utilises the spectral analysis of the phase currents to pinpoint the fault in the machine [6] and to evaluate the load situations. In case an abnormality occurs inside the machine, its frequency components may appear in the current spectrum [7]. Meanwhile, the diagnostic analysis has been reported by sensing currents during transient state and steady-state operation; such as the sequence components of currents, park vectors, wavelet transforms and zero-crossing instants [8-10]. However, these methods suffer from a common drawback: they cannot provide fault location information, nor discriminate between different faults, especially under the influence of power supply and dynamic load variations [11].

Alternatively, vibration can also be a means to detect possible faults developed in electrical machines. Vibration detection techniques are generally effective for detecting mechanical faults, such as bearing failures, gear mesh defects, rotor misalignment and mass unbalance [12, 13]. Their main drawback is that they need detailed information about machine geometry and operating characteristics, such as frequency response functions [14]. In addition, vibration-based monitoring needs expensive sensors to collect the data [15].

Clearly, non-invasive approaches do not disrupt the normal operation of motor drives and are highly desired if they provide reliable condition information where current and mechanical measurements cannot provide. These are technically challenging, but are the focus of this paper. Several research teams have developed condition monitoring technologies by collecting magnetic flux characteristics of machines, as the magnetic flux is related to the magnetic state of the machine, which can be affected by the presence of faults [16]. Since the stray flux is induced by the stator and rotor currents, the stray flux and current signals may provide an insight into the faults and failures in the machines [17]. Moreover, magnetic flux may also provide location information

2

[18] where search coils cannot. Conventional flux-based condition monitoring technologies typically operate under steady-state conditions while transient response analysis can provide dynamic information with a high signal-to-noise ratio [19], Therefore, a time-frequency spectrogram approach is also utilised in this paper in order to obtain load and spectral information associated with faults or failures.

Various magnetic sensors are used for magnetic flux measurements and condition monitoring. There have been several attempts to use search coils to assess for machine monitoring. By implementing search coils into stator slots, any abnormal air-gap flux can been obtained, which presents the health state of electrical machines [20]. However, the search coil monitoring technology is an invasive approach, which may damage the monitored machines. For instance, a loop search coil is developed to be mounted at the machine case to detect the stray flux of the machine. Recent work has focused on the detection of radial magnetic field [21], since the magnetic field can be studied by means of axial and radial direction sensing. By analysing the spectral signatures of stray flux information in the frequency domain, variable types of machine faults can be identified, such as shorted turns, broken bars and end rings in induction machines [21, 22]. However, as the sensitivity of the search coil is at a minimum for low frequencies, a sensitivity problem can arise when a machine is running at low speeds. In recent years, researchers have developed new magnetic flux detection devices to increase measurement sensitivity, response frequency bandwidth and accuracy of monitoring systems [17]. On one hand, a magnetic flux probe was developed with a ferromagnetic core, which leads to an improvement of its characteristics compared with previous search coils [22]. On the other hand, this also gives rise to nonlinearity at high flux amplitude and frequencies. One major disadvantage of coil-based flux measurements is that they cannot measure static magnetic fields due to Faraday's law.

Giant magnetoresistance (GMR) is a relatively new technology for measuring magnetic flux, and is especially suited for measuring low-level stray flux. GMR sensors are built by alternating, thin layers, of magnetic and non- magnetic materials. By applying multiple layer structure, the sensitivity, linearity, spatial resolution and frequency response of GMR sensors are better than search coils [23]. Furthermore, GMR sensors are smaller, cheaper, more flexible and can be easily installed in any machines without causing any disturbance to normal operation. They are initially applied in the field of non-destructive testing and evaluation such as defect detection in ferromagnetic materials and electrical conductors [24-26]. Presently, they are not used for measuring magnetic flux in any electrical machines as a condition monitoring technique.

The paper is organised as follows. Section 2 provides a detailed analysis of using a GMR sensor to measure the static and transient loads of induction motors. Section 3 presents an experimental setup and test results to confirm the effectiveness of the proposed technique, followed by a short conclusion in Section 4.
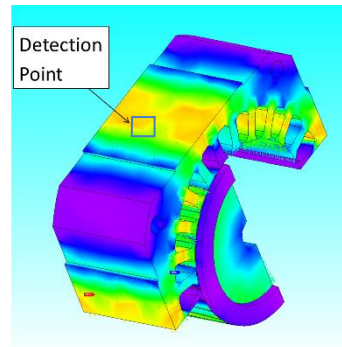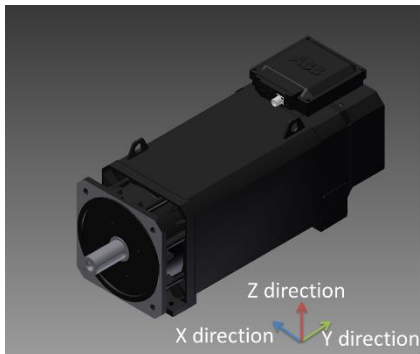
2. Proposed GMR-based load monitoring system

Firstly, an optimised location and direction must be determined. These are studied by Finite element analysis (FEA) simulation.

2.1. Sensor location for measuring stray flux

The stray flux is a magnetic flux that radiates from the inside of the machine frame and is inherently an attenuated air gap flux. It is associated with stator and rotor currents; both produce magnetic flux with different spectral components. Depending on the physical location of the measurement point, the stray flux can contain information about both stator- and rotor-producing fields to a varying degree.

In order to select sensor specifications and appropriate locations for installing the GMR sensors, FEM simulation on a targeted motor is carried out. Fig. 1*a* shows a FEA model and Fig. 1*b* shows the 3D distribution of the magnetic field. Fig. 1*c* presents the magnetic flux lines distributions outside the cage. From the simulation results, the strongest stray flux and most significant magnetic field change occur in the centre of the machine case, as highlighted in Fig. 1*b*. Fig. 1*d* illustrates three different directions and their variations at the optimised location, where the z-direction provides the strongest magnetic flux (5 m*T*). Stray flux is a reflection of the air-gap flux which is attenuated by the stator laminations and machine frame. There are two potential sensor locations, which are around the shaft at the end of motor and at the mid point of the machine cage. Nonetheless, the stray flux at the machine ends is also influenced by the endwindings. Thus, the stray flux at the middle of the machines is chosen as the GMR sensor location. From numerical results, this is the axial mid-point in the z-direction.
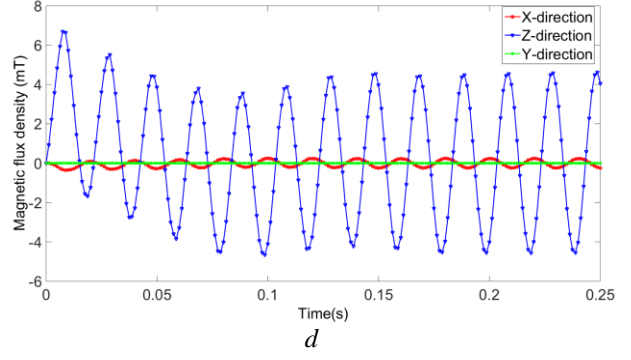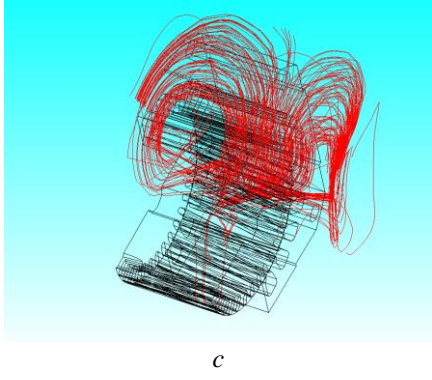

a

b

c

d

Fig. 1. *Simulation results of the target induction machine*
a FEA model of the tested induction machine
b Magnetic field distribution of the machine
c Magnet field flux distribution outside the machine
d Magnetic flux density in three directions

2.2. *Principles of the proposed load monitoring system*

The relationships of stator- and rotor-current-induced magnetic fluxes and motor load torque are presented as follows.

The stray flux of an induction machine is created by both stator and rotor currents. The reference frames can be transformed from the 3 phase (*a-b-c* axis) to the *d-q* axis using the Clarke transformation, and then to the $\gamma - \delta$ axis by the Park transformation. In this case, the air gap flux is used to link the stray flux with motor load. This air-gap flux can be expressed as [27]:

$$\Psi_{rg} = M i_{\gamma s} + M_{\gamma r} \tag{1}$$

$$\Psi_{\delta g} = M i_{\delta s} + M_{\delta r} \tag{2}$$

where subscripts *r* and δ indicate the rotor and stator components, respectively. Ψ_g is the air-gap flux; *M* is the mutual inductance. $i_{\gamma s}, i_{\delta s}$ are the stator currents in the $\gamma - \delta$ axis and $i_{\gamma r}, i_{\delta s}$ are the rotor currents in the $\gamma - \delta$ axis, respectively.

From equations (1 and 2), both the stator current and rotor current affect the magnetic field in the air gap. The air gap flux is given by:

$$B_{out} = \sum_{k,m} B \sin(K\omega t - m\phi - \varphi_{k,m}) \tag{3}$$

where *B* is the component magnitude, B_{out} is the magnetic flux density in the air gap at a given point, *m* is the number of pole pairs, ω is the angular speed, *k* is the harmonic rank, ϕ is the angular position, $\varphi_{k,m}$ is the initial phase. From numerical analysis, the relationship of the radial magnetic flux density and the air-gap flux density is linear. Fig. 2 shows the stray flux within an induction motor.
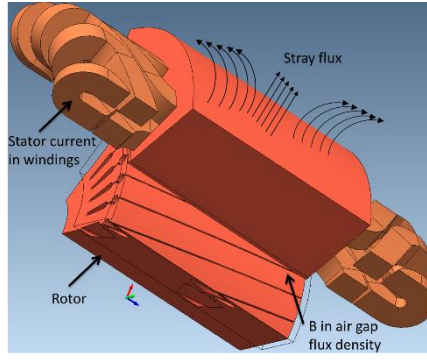
Fig. 2. *The stray flux in an induction machine*

As discussed in [17, 28], the radial external magnetic field is related to the air gap flux in the way it is attenuated by the stator lamination and the external machine yoke. The attenuation phenomena can be decoupled and calculated by using a global transmission coefficient. The global attenuation coefficient (K_H) can be determined by multiplying individual attenuation coefficients of the stator yoke, machine frame and the air gap between the case and the sensor [29, 30].

For a field-oriented induction motor drive, its torque is calculated by

$$T_e = \left(\frac{3}{4} P \frac{L_m^2}{L_{rr}} i_{ds} \right) \; i_{qs} = K_t i_{qs} \tag{4}$$

where L_m is the stator-rotor mutual inductance and L_{rr} is the rotor self-inductance.

Considering the load and disturbance, the motor torque can be rewritten as

$$T_e = (T_L + \Delta T) + B\omega_r + J\frac{d\omega_r}{dt} \tag{5}$$

where T_L is the load torque, ΔT is torque disturbance, B is the friction factor of the bearings, and J is the total mechanical inertia constant of the motor and load.

Thus the whole drive system can be represented by the control system block diagram as shown in Fig. 3. In the model of variable speed drive dynamics, an induction machine generates electromagnetic torque T_e according to the torque current i_{qs} from speed controller.
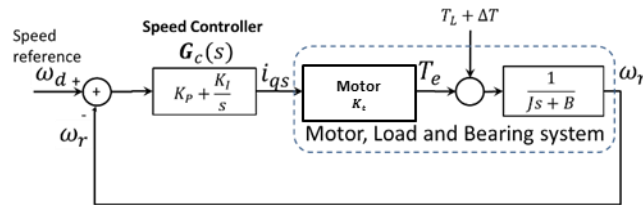

Fig. 1. *System model of the induction motor drive*

The close loop transfer function from speed reference $\Omega_d(s)$ to the rotor speed $\Omega_r(s)$ is given by

$$G(s) = \frac{\Omega_r(s)}{\Omega_d(s)} = \frac{G_c(s)G_p(s)}{1+G_c(s)G_p(s)} \tag{6}$$

where the capital letters denote the Laplace transformation of corresponding parameters.

By algebraic manipulation, the close loop transfer function can be rewritten as a 2nd-order dynamic system with one zero.

$$G(s) = \frac{\frac{K_t K_I}{J}\left(\frac{K_P}{K_I}s+1\right)}{s^2+\frac{K_t K_P+B}{J}s+\frac{K_t K_I}{J}} \tag{7}$$

Let $K_P = \frac{2\zeta\omega_0-a}{b}$ and $K_I = \frac{\omega_0^2}{b}$, we have $a + bK_P = 2\zeta\omega_0$ and $bK_I = \omega_0^2$. Therefore,

$$G(s) = \frac{\omega_0^2}{s^2+2\zeta\omega_0 s+\omega_0^2} + \frac{2\zeta}{\omega_0} \cdot \frac{\omega_0^2 s}{s^2+2\zeta\omega_0 s+\omega_0^2} \tag{8}$$

Let $h_0(t)$ be the unit step response of the transfer function.

$$G_0(s) = \frac{\omega_0^2}{s^2+2\zeta\omega_0 s+\omega_0^2} \tag{9}$$

$$h_0(t) = \left\{1 - e^{-\zeta\omega_0 t}\left(\cos(\omega_0\sqrt{1-\zeta^2}t) + \frac{\zeta}{\sqrt{1-\zeta^2}}\text{sen}(\omega_0\sqrt{1-\zeta^2}t)\right)\right\} \tag{10}$$

Usually, $\zeta = 1$ in order to achieve critical damping, the step response of $G(s)$ is

$$h(t) = h_0(t) + \frac{2\zeta}{\omega_0} \cdot \frac{dh_0(t)}{dt} == 1 + e^{-\omega_0 t}(\omega_0 t - 1) \tag{11}$$

As the machine load increases, the damping factor ζ increases. This will slow down the system's unit step response and gives rise to its time constant.

It becomes clear that measuring the magnetic flux helps trace the stator or current variations which link with load variations. As magnetic sensors have high-frequency response, the transient magnetic field is also needed in order to monitor dynamic loads, which will be discussed in Section 3.

3. Experimental Studies

The proposed GMR-based load monitoring system is implemented experimentally so as to illustrate the relationship between load variations and measured stray flux in steady and transient states. Two experimental test benches have been developed to perform a motor load test and a bearing test, as shown in Fig. 4. Firstly, two identical 1.5 kW induction motors are tested on the motor load bench to verify the repeatability of the test method. Their stator windings are star connected and the rotor windings are short-circuited. The frame of the test induction machines is aluminium. The load is a DC motor coupled to the test machine shaft and controlled by a DC load drive. Furthermore, a torque meter, an encoder and a power analyzer are employed to measure load torque, speed, load and output power, as shown in Fig. 4a and Fig. 4c. A GMR sensor (NVE AA002) is glued in the middle of the machine yoke to measure the stray magnetic flux. The output voltage from the GMR sensor is measured by an oscilloscope and recorded on a PC.

Experimental work is carried out via no-load, static and dynamic load tests, in the first test bench. During the no-load test, the machine is operated at the synchronous speed. After that, one DC motor provides a constant load to the test machine. In the dynamic load test, the DC motor applies a constant load and the stray magnetic flux is measured from the machine start-up process up to a steady-state operation.

The bearing test bench is used to investigate the fatigue progress in a bearing driven by the third induction machine. This is a three-phase 59 kW wound rotor induction machine with a steel frame. By using a hydraulic system, variable loads can be applied to the test bearing to accelerate the ageing of the bearing. With the degradation of the test bearing, the motor load would increase to some degree, which is detected by the GMR sensor.
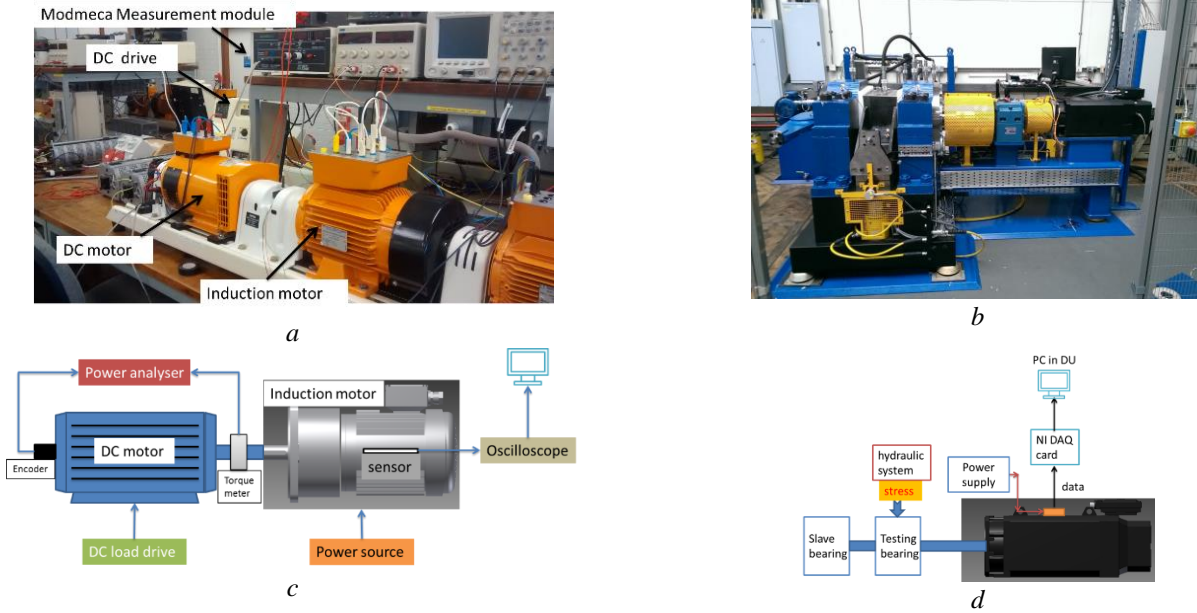

Fig. 4. *Induction machine load monitoring test benches*
a Photograph of the motor load test bench
b Photograph of the bearing test bench
c Schematic of the motor load test bench
d Schematic of the bearing test bench

The magnetic flux data are analysed in two different approaches. From the motor load test, the test results are analysed by comparing their amplitudes. The magnetic sensor data during machine start-up are analysed in the time-frequency spectrum. By monitoring changes in the stray flux, the change in dynamic load can be observed.

Steady and transient features are extracted by analysing the magnetic stray flux data. The peak values of magnetic stray flux from steady state test results are calculated. The spectrograms illustrate the transient information of the magnetic stray flux. The spectrogram provides patterns to estimate the harmonic contents of a time-varying signal, which helps develop a visual correlation of load variations and detected signals. The spectrogram is a square modulus of the fixed widowed Fourier transform of a signal:

$$S_x(t,v) = \left| \int_{-\infty}^{+\infty} x(s) * h(s-t) * e^{-i*2\pi vs} ds \right| \tag{12}$$

where $x(s)$ is the temporal signal, $h(s-t)$ is the window conjugate form and v is the frequency. By applying the short-time Fourier transform (STFT) on the test data, transient information of the test data is obtained in the time-frequency domain.

3.1. Steady state test result and data analysis

At the motor load test, the DC motor generates loads ranging from 0 to 5 N·m. The stray flux is measured in the z-direction of magnetic field on the machine frame. The GMR sensor detects the radial magnetic flux of external magnetic field of the test machine. The output voltage waveform of the GMR sensor is almost sinusoidal in Fig. 5a.
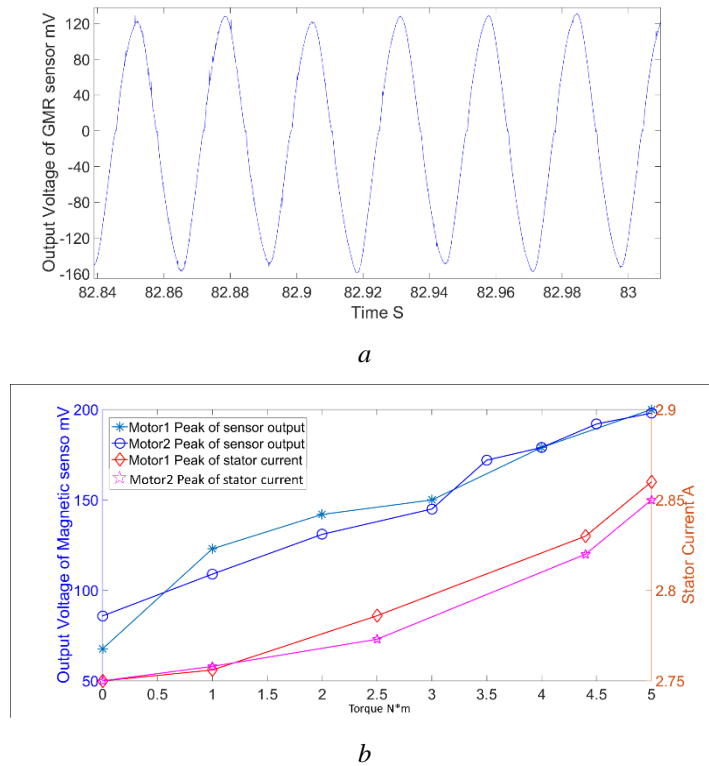

a

b

Fig. 5. *Stator current and peak values of the GMR output under different loads*
a GMR sensor voltage output waveform
b Comparisons of stator current and peak values of the GMR sensor output under different loads

Different steady features are captured, as presented in Fig. 5b. It can be seen that the stray flux increases with loading in a steady state operation; and its peak value increases from 68.1 to 198 mV and 87.1 to 200mV, respectively. In Fig. 5b, the stator current is also shown. From the previous analysis in Section 1, the stator current can increase the stray magnetic flux which is measured in the z-direction around the machine in this study. As a result, the load state of the induction machine can be monitored by GMR sensor in the steady state.

3.2. Transient test result and data analysis

The transient state of the machine loading can also be monitored through two different indicators. They are the first peak value of the GMR voltage output waveform, and the transient response time of spectrogram results. Fig. 6 shows the measured output voltage waveforms from the GMR sensor during two machine operational conditions. By controlling the DC motor as a variable load, the test machine starts with a fixed load while the load changes from 5, 4.5, 4, 3.5, 3, 2 to 1 N·m for starting tests. Test results are presented in Fig. 6. It is observed that there is a peak value at around 80 mS in every waveform of the stray magnet flux and the peak value of this waveform increases with loads. The air-gap magnetic flux reaches a maximum value at the beginning of the start-up period. It is evident that the stray flux can indicate the load variations in the machine starting transients.
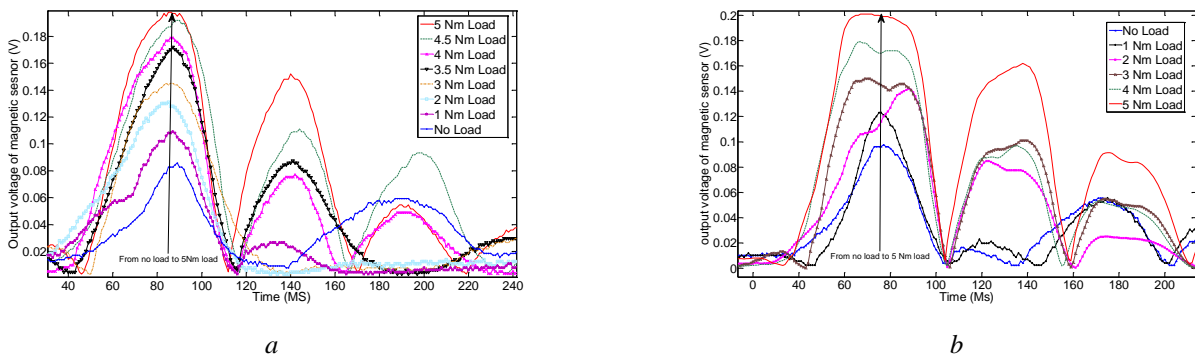

| *a* | *b* |

Fig. 6. *Results of motors 1 and 2*

a Induced voltage of the GMR sensor during starting-up of motor 1

b Induced voltage of the GMR sensor during starting-up of motor 2

In order to investigate the repeatability of the proposed load monitoring method, two identical induction motors were tested in the experiment, as illustrated in Fig. 6*a* and Fig. 6*b*. It can be seen in Fig. 6*a* that their first peaks and transient response times have the same trends as the load varies. Their ~~individual~~ machine characteristics can be compared by ~~transient responses e.g.~~ the time-spectrograph analysis, as shown in Fig. 7.

The output results for start-up are illustrated in the time-frequency domain in Fig. 7. The transient response time is the time from the machine start point to the steady state. Whenever test machine starts, there is a trigger signal sent from machine control board to the NI DAQ card. Additionally, from the spectrogram, the time entered into steady state can be found. Thus, by calculating the difference between the two, the transient response time is obtained. As discussed in Section 2.1, the load variations will lead the changing of transient time during the start-up of induction machines. In this case, as the load torque increases, the transient response time of induction motors rise to meet the same speed with the previous load situation. Fig. 7*a* and Fig. 7*b* illustrate the spectrograms of magnetic sensor signals during the motor start-up. In particular, at the beginning of the start-up

transient time, the spectrum results demonstrate significant variations, as illustrated in Fig 7. Fig. 7*a* and Fig. 7*b* show a slight difference in the spectrograms of the two motors during starting-up.

The comparison between the GMR sensor output in a steady state and the transient response time in a transient state are illustrated in Fig. 7*c*. The transient response time is more sensitive than the peak value to detect the load variation. From Fig.7*c*, the slope of the transient response time is greater than the peak value during load variations, which leads to better performance of the monitoring system. The peak value data are captured during the steady state, and the response time is collected in the transient state. The transient state can be considered as a collection of numerous steady states, which contains richer information than the steady-state data. Thus, the transient response time can provide better sensitivity performance than the peak values to monitor load variation.
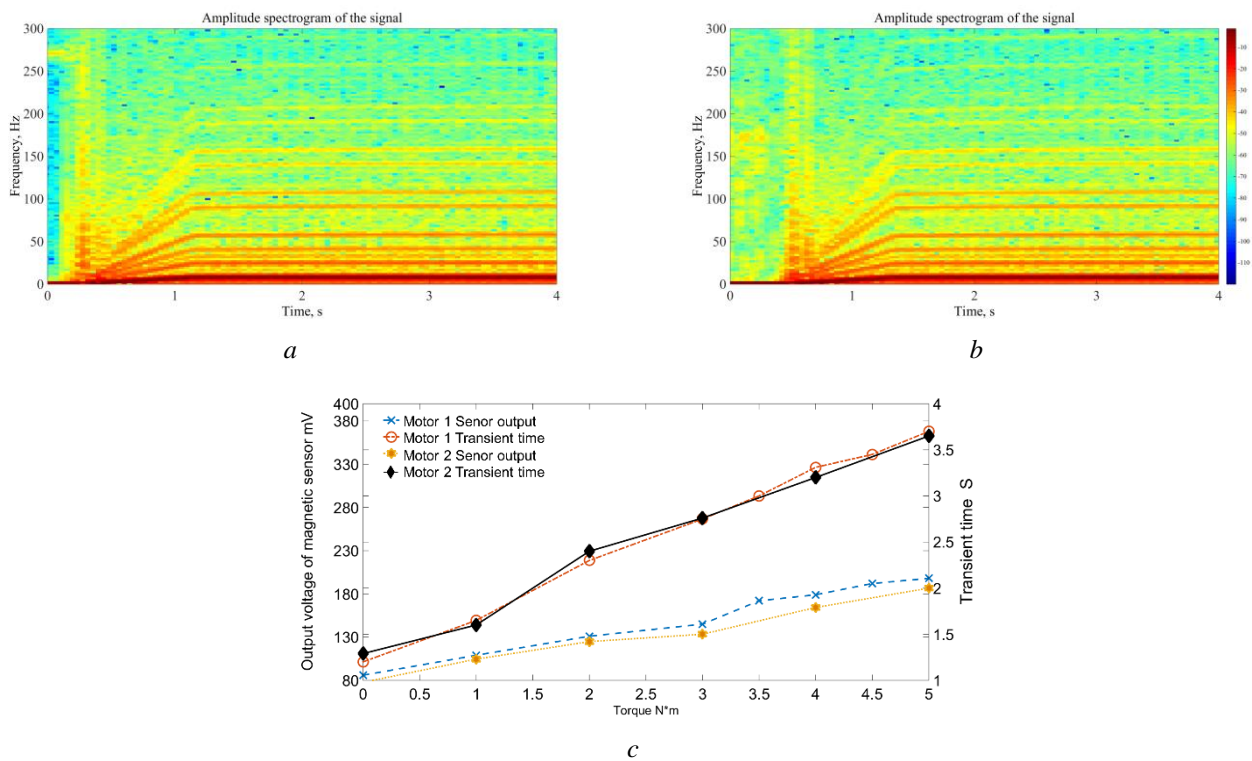

a

b

c

Fig. 7. *Spectrograms of the GMR sensor outputs in the time-frequency domain*
a Motor 1 spectrogram for start-up
b Motor 2 spectrogram for start-up
c Comparison of the peak value and transient response time during starting up

To validate the proposed method and feature extraction for monitoring induction machines, the second load monitoring test was applied to a 59 kW motor. The first case study was carried out with steady features applied. As shown in the bearing test bench (Fig. 4*b*), the motor shaft is directly linked with a test bearing. As the hydraulic system exerts an additional constant load on the bearing, bearing cracks or failures may be generated as a result of excessive fatigue cycling. Any cracks and faults on the

test bearing will lead to a load increase. The proposed method and transient feature (spectrogram) were applied to load monitoring, especially at motor start-up for estimating the bearing condition. Fig. 8*a* and Fig.8*b* show the bearing state (outer race and inner race) before and after a ten-day accelerated fatigue test. The test data from the second test bench was processed and the spectrogram results are shown in Fig. 8*c*. The start-up process is divided into several steps due to the heavy load and large power rating of the experimental system. After several days of continuous testing, the start transient response time was obtained and plotted in Fig. 8*d*. As the transient response time increases, some bearing faults start to appear, as illustrated in Fig. 8*b*. It is thus proven that the spectrogram (transient response time in particular) is a valid feature to monitor the bearing fatigue.
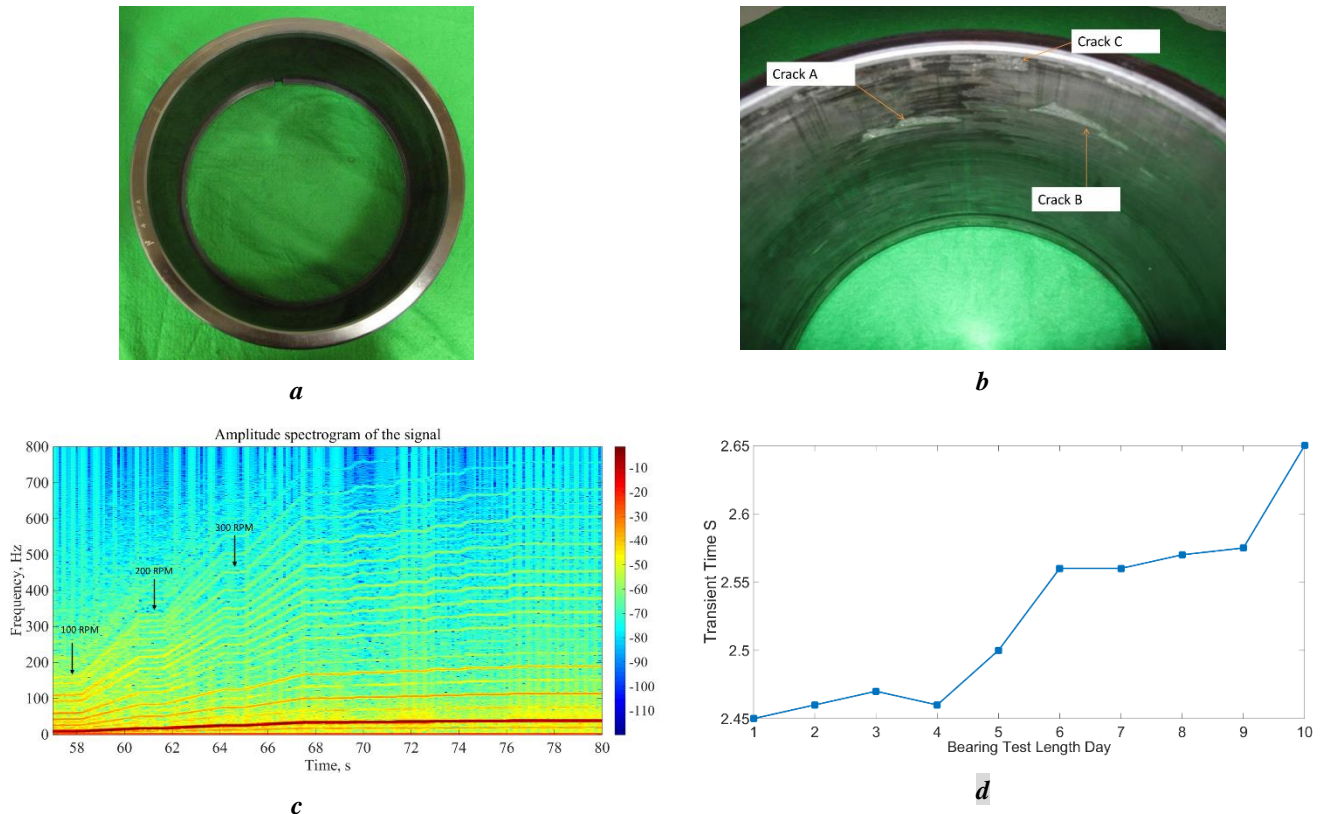

Fig. 8 *The test bearing status in the experiment*

a Bearing race before bearing test

b Scratch on the test bearing

c Data analysis by using STFT in spectrogram

d Transient time during the experiment

4. Conclusions

In this paper, a new non-invasive load monitoring method has been proposed by measuring the external magnetic flux outside of the machine frame, based on a GMR magnetic sensor with spectrogram's information. The GMR sensor monitoring

system offers excellent spectral responses, making it suitable for evaluating both transient and steady-state performance of induction motors.

From the simulation results, the optimised sensor location and detection direction are firstly determined. The best location is found in the radial direction of the mid-point of the test machine. Steady/transient magnetic field measurements and feature analysis have been conducted at varying load conditions.

Experimental studies have been carried out through steady and transient magnetic field measurements. In a steady state operation, the steady features are applied for load monitoring and feature extraction. When induction motors start up with loads, the first peak of the output voltage of the magnetic sensor is a good indicator. Secondly, the spectrogram is used to provide patterns between time and frequency. By referencing the transient time information of the stray flux spectrogram patterns, the load variations can be illustrated during the experiments. Compared with steady state analysis, the transient response time can provide more effective and better results for the dynamic load states. Overall, experimental tests on three induction motors have confirmed the effectiveness of the proposed method for load monitoring.

5.   Acknowledgments

6.   References

1. Cao, W.P., Bradley, K.J.: 'Assessing the impacts of rewind and repeated rewinds on induction motors: is an opportunity for Re-designing the machine being wasted?', *IEEE Trans. Ind. Appl.,* 2006, **42**, (4), pp. 958-964
2. Tavner, P. J.: 'Review of condition monitoring of rotating electrical machines', *IET Electr. Power Appl.*, 2008, **2**, (4), pp. 215-247
3. Kerres, B., Fischer, K., Madlener, R.: 'Economic evaluation of maintenance strategies for wind turbines: a stochastic analysis,' *IET Renew. Power Gener.*, 2015, **9**, (7), pp. 766-774
4. Djurovic, S., Crabtree, C. J., Tavner, P. J., Smith, A. C.: 'Condition monitoring of wind turbine induction generators with rotor electrical asymmetry', *IET Renew. Power Gener.*, 2012, **6**, (4), pp. 207-216
5. Salles, G., Filippetti, F., Tassoni, C., Crellet, G., Franceschini, G.: 'Monitoring of induction motor load by neural network techniques', *IEEE Trans. Power Electron.,* 2000, **15**, (4), pp. 762-768
6. Ebrahimi, B. M., Roshtkhari, M. J., Faiz, J., Khatami, S. V.: 'Advanced eccentricity fault recognition in permanent magnet synchronous motors using stator current signature analysis'. *IEEE Trans. Ind. Electron.*, 2014, **61**, (4), pp. 2041-2052
7. Thomson, W. T., Fenger, M.: 'Current signature analysis to detect induction motor faults', *IEEE Trans. Ind. Appl.*, 2001, **7**, pp. 26-34
8. Zhang, P., Du, Y., Habetler, T. G., Lu, B.: 'A survey of condition monitoring and protection methods for medium-voltage induction motors', *IEEE Trans. Ind. Appl.*, 2011, **47**, (1), pp. 34-46
9. Seshadrinath, J., Singh, B., Panigrahi, B. K.: 'Incipient turn fault detection and condition monitoring of induction machine using analytical wavelet transform', *IEEE Trans. Ind. Appl.*, 2014, **50**, (3), pp. 2235-2242
10. Nejjari, H., Benbouzid, M. E. H.: 'Monitoring and diagnosis of induction motors electrical faults using a current Park's vector pattern learning approach', *IEEE Trans. Ind. Appl.*, 2000, **36**, (3), pp. 730-735
11. Frosini, L., Borin, A., Girometta, L., Venchi, G.: 'A novel approach to detect short circuits in low voltage induction motor by stray flux measurement', *Proc. Int. Conf. Electrical Machines (ICEM)*, Marseille, France, 2012, pp. 1538-1544
12. Filho, L. P. C. M., Pederiva, R., Brito, J. N.: 'Detection of stator winding faults in induction machines using flux and vibration analysis', *Mechanical Systems and Signal Processing*, 2014, **42**, (1), pp. 377-387

13. Gritli, Y., Tommaso, A. O., Filippetti, F., Miceli, R., Rossi,C., Chatti, A.: 'Investigation of motor current signature and vibration analysis for diagnosing rotor broken bars in double cage induction motors', *Proc. Int. Conf. Power Electronics, Electrical Drives, Automation and Motion (SPEEDAM)*, Sorrento, Italy, 2012, pp. 1360-1365

14. Seshadrinath, J., Singh, B., Panigrahi, B. K.: 'Vibration analysis based interturn fault diagnosis in induction machines', *IEEE Trans. Ind. Informat.*, 2014, **10**, (1), pp. 340-350

15. Frosini, L., Harlisca, C., Szabó, L.: 'Induction machine bearing faults detection by means of statistical processing of the stray flux measurement', *IEEE Trans. Ind. Electron.*, 2015, **62**, (3), pp.1846-1854

16. Henao, H., Demian, C., Capolino, G. A.: 'A frequency-domain detection of stator winding faults in induction machines using an external flux sensor', *IEEE Trans. Ind. Appl.*, 2003, **39**, (5), pp. 1272-1279

17. Romary, R., Pusca, R., Lecointe, J. P., Brudny, J. F.: 'Electrical machines fault diagnosis by stray flux analysis', *Proc. Int. Conf. Electrical Machines Design, Control and Diagnosis (Wemdcd)*, Paris, France, 2013, pp. 247-256

18. Pusca, R., Romary, R., Ceban, A., Brudny, J. F.: 'An online universal diagnosis procedure using two external flux sensors applied to the ac electrical rotating machines', *Sensors*, 2010, **10**, (11), pp. 10448-10466

19. Ruqiang, Y., Gao, R. X.: 'Hilbert-Huang Transform-Based Vibration Signal Analysis for Machine Health Monitoring', *IEEE Trans. Instrum. Meas.*, 2006, **55**, (6), pp. 2320-2329

20. Negrea, M. D.: "Electromagnetic flux monitoring for detecting faults in electrical machines," PhD thesis, Helsinki University of Technology, 2006

21. Kokko, V.: "Condition monitoring of squirrel-cage motors by axial magnetic flux measurements," PhD thesis, University of Oulu, 2003

22. Frosini, L., Borin, A., Albini, A., Benzi, F.: 'New techniques to simulate and diagnose stator winding faults in low voltage induction motors', *Proc. Int. Conf. Electrical Machines (ICEM)*, Marseille, France, 2012, pp. 1783-1789

23. Schneider, P. E., Horio, M., Lorenz, R. D.: 'Integrating GMR field detectors for high-bandwidth current sensing in power electronic modules', *IEEE Trans. Ind. Appl.*, 2012, **48**, (4), pp. 1432-1439

24. Kral, J., Smid, R., Ramos, H. M. G., Ribeiro, A. L.: 'The lift-off effect in eddy currents on thickness modeling and measurement', *IEEE Trans. Instrum. Meas.*, 2013, **62**, (7), pp. 2043-2049

25. Wilson, J. W., Tian, G. Y.: 'Pulsed electromagnetic methods for defect detection and characterisation', *NDT & E International*, 2007, **40**, (4), pp. 275-283

26. Wilson, J. W., Tian, G. Y., Barrans, S.: 'Residual magnetic field sensing for stress measurement', *Sensors and Actuators A: Physical*, 2007, **135**, (2), pp. 381-387

27. Suzuki, T., Chiba, A., Rahman, M. A., Fukao, T.: 'An air-gap-flux-oriented vector controller for stable operation of bearingless induction motors', *IEEE Trans. Ind. Appl.*, 2000, **36**, (4), pp. 1069-1076

28. Du, Y., Cheng, T. C., Farag, A. S.: 'Principles of power-frequency magnetic field shielding with flat sheets in a source of long conductors', *IEEE Trans. Electromagn. Compat.*, 1996, **38**, (3), pp. 450-459

29. Romary, R., Roger, D., Brudny, J. F.: 'Analytical computation of an AC machine external magnetic field', *The European Physical Journal Applied Physics*, 2009, **47**, (3), pp. 311-321

30. Wiak, S., Krawczyk, A., Dolezel, I., Thailly, D., Romary, R., Roger, D., Brudny, J. F.: 'Attenuation of magnetic field components through an AC machine stator', *The international journal for computation and mathematics in electrical and electronic engineering*, 2008, **27**, (4), pp. 744-753